



This discussion paper is/has been under review for the journal Geoscientific Model Development (GMD). Please refer to the corresponding final paper in GMD if available.

Ice-sheet configuration in the CMIP5/PMIP3 Last Glacial Maximum experiments

A. Abe-Ouchi^{1,2}, F. Saito², M. Kageyama³, P. Braconnot³, S. P. Harrison⁴,
K. Lambeck⁵, B. L. Otto-Bliesner⁶, W. R. Peltier⁷, L. Tarasov⁸, J.-Y. Peterschmitt³,
and K. Takahashi²

¹Atmosphere Ocean Research Institute, University of Tokyo, 5-1-5, Kashiwanoha, Kashiwa-shi, Chiba 277-8564, Japan

²Japan Agency for Marine-Earth Science and Technology, 3173-25 Showamachi, Kanazawa, Yokohama, Kanagawa, 236-0001, Japan

³Laboratoire des Sciences du Climat et de l'Environnement/Institut Pierre Simon Laplace unité mixte de recherches CEA-CNRS-UVSQ, Orme des Merisiers, point courrier 129, 91191 Gif sur Yvette Cedex, France

⁴Centre for Past Climate Change and School of Archaeology, Geography and Environmental Sciences, University of Reading, Whiteknights, Reading, RG6 6AH, UK

⁵Research School of Earth Sciences, The Australian National University, Canberra, ACT 0200, Australia

⁶Climate and Global Dynamics Division, National Center for Atmospheric Research, Boulder, CO 80305, USA

Title Page

Abstract

Introduction

Conclusions

References

Tables

Figures



Back

Close

Full Screen / Esc

Printer-friendly Version

Interactive Discussion



⁷Department of Physics, University of Toronto, 60 George Street, Toronto, Ontario, M5S 1A7, Canada

⁸Department of Physics and Physical Oceanography, Memorial University of Newfoundland, St. John's, NL A1B 3X7, Canada

Received: 28 April 2015 – Accepted: 11 May 2015 – Published: 3 June 2015

Correspondence to: A. Abe-Ouchi (abeouchi@aori.u-tokyo.ac.jp)

Published by Copernicus Publications on behalf of the European Geosciences Union.

GMDD

8, 4293–4336, 2015

PMIP3 Ice sheet configuration

A. Abe-Ouchi et al.

Title Page

Abstract

Introduction

Conclusions

References

Tables

Figures



Back

Close

Full Screen / Esc

Printer-friendly Version

Interactive Discussion



Abstract

We describe the creation of boundary conditions related to the presence of ice sheets, including ice sheet extent and height, ice shelf extent, and the distribution and altitude of ice-free land, at the Last Glacial Maximum (LGM) for use in LGM experiments conducted as part of the fifth phase of the Coupled Modelling Intercomparison Project (CMIP5) and the third phase of the Palaeoclimate Modelling Intercomparison Project (PMIP3). The CMIP5/PMIP3 data sets were created from reconstructions made by three different groups, which were all obtained using a model-inversion approach but differ in the assumptions used in the modelling and in the type of data used as constraints. The ice sheet extent, and thus the albedo mask, for the Northern Hemisphere (NH) does not vary substantially between the three individual data sources. The difference in the topography of the NH ice sheets is also moderate, and smaller than the differences between these reconstructions (and the resultant composite reconstruction) and ice-sheet reconstructions used in previous generations of PMIP. Only two of the individual reconstructions provide information for Antarctica. The discrepancy between these two reconstructions is larger than the difference for the NH ice sheets although still less than the difference between the composite reconstruction and previous PMIP ice-sheet reconstructions. Differences in the climate response to the individual LGM reconstructions, and between these reconstructions and the CMIP5/PMIP3 composite, are largely confined to the ice-covered regions, but also extend over North Atlantic Ocean and Northern Hemisphere continents through atmospheric stationary waves. There are much larger differences in the climate response to the latest reconstructions (or the derived composite) and ice-sheet reconstructions used in previous phases of PMIP.

PMIP3 Ice sheet configuration

A. Abe-Ouchi et al.

Title Page

Abstract

Introduction

Conclusions

References

Tables

Figures



Back

Close

Full Screen / Esc

Printer-friendly Version

Interactive Discussion



1 Introduction

There are large differences in the modelled response to scenarios of future climate forcing (Kirtman et al., 2013; Collins et al., 2013). Modelling of past climate states, and evaluation of the simulations using palaeoclimate reconstructions, provides an opportunity to quantify and to explore the causes of these uncertainties (Braconnot et al., 2012; Masson-Delmotte et al., 2013; Schmidt et al., 2014). The Last Glacial Maximum (LGM, ca. 21 000 yr BP) is an exemplary period for such an exercise because the change in global forcing was large and, although the forcing was different in nature, the magnitude is equivalent to that expected by the end of the 21st century (Braconnot et al., 2012). The LGM has been a major focus for simulations since the early days of numerical modelling (e.g. Aleya, 1972; Williams et al., 1974; Gates, 1976; Manabe and Hahn, 1977; Kutzbach and Guetter, 1986), and was chosen as a focus for model experiments carried out in both Phase 1 and Phase 2 of the Palaeoclimate Modelling Intercomparison Project (PMIP: Braconnot et al., 2007a, b) because of the availability of syntheses of palaeoclimatic reconstructions (e.g. MARGO Project Members, 2009; Bartlein et al., 2011; Schmittner et al., 2011; Braconnot et al., 2012) for model evaluation. It is perhaps not surprising then that the LGM was one of the simulations chosen when palaeoclimate experiments were first included in the fifth phase of the Coupled Modelling Intercomparison Project (CMIP5: Taylor et al., 2011; Braconnot et al., 2012). The LGM simulations are further examined to constrain the climate sensitivity, which is an important metrics for the future climate projection (Masson-Delmotte et al., 2006, 2013; Hargreaves et al., 2007; Yoshimori et al., 2009, 2011; Brady et al., 2013).

The boundary conditions that must be specified for the LGM experiment are a (relatively small) change in orbital forcing, reduced atmospheric concentrations of greenhouse gases, and the presence of large ice sheets. Land-surface conditions, in particular the distribution of vegetation (Prentice et al., 2000; Harrison and Bartlein, 2012), were also different at the LGM. However, the spatial coverage of information on LGM vegetation is currently insufficient to provide a gridded global data set to use as a model

GMDD

8, 4293–4336, 2015

PMIP3 Ice sheet configuration

A. Abe-Ouchi et al.

Title Page

Abstract

Introduction

Conclusions

References

Tables

Figures



Back

Close

Full Screen / Esc

Printer-friendly Version

Interactive Discussion



PMIP3 Ice sheet configuration

A. Abe-Ouchi et al.

Title Page

Abstract

Introduction

Conclusions

References

Tables

Figures

◀

▶

◀

▶

Back

Close

Full Screen / Esc

Printer-friendly Version

Interactive Discussion



input. LGM vegetation was therefore either computed by the model or prescribed to be the same as the pre-industrial control simulation. However, the changes in orbital forcing and greenhouse gas concentrations are well known. The expansion of the ice sheets at the LGM resulted in a sea-level lowering of ca 130 m and changed palaeogeography. The marginal limits of the North American (Laurentide), Greenland and European ice sheets are increasingly well constrained by radiocarbon dated moraines and other glacial deposits (e.g. Dyke and Prest, 1987; Mickelson and Colgan, 2003; Dyke, 2004; Gyllencreutz et al., 2007; Simpson et al., 2009; Ehlers et al., 2011; Mangerud et al., 2013). However, there is little direct evidence for the distribution of ice mass, and this must therefore be inferred through a combination of physical modelling and the use of indirect observational constraints (such as information on relative sea level changes). Thus, the specification of the overall form of the ice sheets has been a major source of uncertainty in defining boundary conditions for LGM experiments.

The earliest LGM simulations made use of a reconstruction of ice sheet extent and height made by the CLIMAP project (CLIMAP Project Members, 1976; CLIMAP, 1981). Subsequently, the PMIP project made use of reconstructions based on two different generations of an isostatic rebound model: ICE-4G (Peltier, 1994) in the first phase of the project (PMIP1) and ICE-5G v1.1 in PMIP2 (Peltier, 2004). The inferred ice volume was ca 35 % lower in ICE-4G than in the earlier CLIMAP reconstructions, resulting in considerably lower maximum elevations for the Laurentide and European ice sheets. The Laurentide has greater volume in ICE-5G than ICE-4G, and the Keewatin Dome is 2–3 km higher over much of central Canada, but the European Ice sheet is less extensive in ICE-5G than ICE-4G.

The lowering of CO₂ makes a large contribution to the cooling at the LGM (Broccoli and Manabe, 1987; Hewitt and Mitchell, 1997; Broccoli, 2000; Kim, 2004; Otto-Bliesner et al., 2006; Brady et al., 2013), but the ice sheets (and the changes in albedo caused by the change in land-sea geography associated with the growth of these ice sheets and lowering of sea level) also have an important impact on both regional and global climates, particularly in the NH. Furthermore, the change in land-sea geography has

PMIP3 Ice sheet configuration

A. Abe-Ouchi et al.

Title Page

Abstract

Introduction

Conclusions

References

Tables

Figures

◀

▶

◀

▶

Back

Close

Full Screen / Esc

Printer-friendly Version

Interactive Discussion



impacts on sea level and ocean circulation which directly affects the carbon cycle, atmospheric CO₂ concentrations and the glacial cycles (Brovkin et al., 2012; Ganopolski and Calov, 2011; Abe-Ouchi et al., 2013). The magnitude of impacts on both the radiation balance (via albedo and lapse rate effect) and atmospheric circulation (planetary stationary wave, location of storm tracks), and the impact on the ocean, are all particularly sensitive to differences in the specification of ice-sheet height, and indeed simulations using different ice sheet configurations have demonstrated large differences both in global mean temperature and in NH circulation patterns and regional temperatures (Justino et al., 2005; Otto-Bliesner et al., 2006; Abe-Ouchi et al., 2007; Clark et al., 2009; Pausata et al., 2011; Vettoretti and Peltier, 2013; Ullman et al., 2014).

At the time of the definition of the PMIP3 boundary conditions, there were several candidate ice-sheet reconstructions that could have been used as a boundary condition for the CMIP5/PMIP3 LGM simulations (ICE-6G v2.0: Argus and Peltier, 2010; GLAC-1a: Tarasov et al., 2012; ANU: Lambeck et al., 2010), which differ in the assumptions used in the modelling and in the type of data used as constraints on these models. The purpose of this paper is to explain the ice-sheet configuration that was used in the CMIP5/PMIP3 simulations, which was created by blending the three individual realisations, and to explore the consequences of this choice. The individual ice sheet reconstructions are described in Sect. 2, and the procedure for creating the blended ice sheet is described in Sect. 3. The differences between this blended ice sheet, the individual ice sheet reconstructions, and previous ice sheet configurations used by PMIP, and their impact on forcing and climate, are discussed in Sect. 4. The final section of the paper highlights the uncertainties associated with the specification of the CMIP5/PMIP3 ice sheet and makes recommendations for further work to minimise these uncertainties.

2 Documentation of the original ice-sheet reconstructions

2.1 ICE-6G v2.0 ice reconstruction

ICE-6G is the latest of a series of inversions of a glacial isostatic adjustment (GIA) model based on the solution for the impulse response of a viscoelastic Earth to surface loading described by Peltier (1974), in which global ice history and radial Earth viscosity profiles are repeatedly tuned to improve model predictions of relative sea-level (RSL) histories and present-day deformation rates compared to observations (Peltier and Andrews, 1976; Peltier, 1976; Tushingham and Peltier, 1991; Peltier, 1994, 2002, 2004; Argus and Peltier, 2010; Engelhart et al., 2011). The model is based upon detailed and continuously updated analyses of data of each of the previously glaciated regions (North America: Peltier, 2004; Argus and Peltier, 2010; Fennoscandia: Peltier, 2004; Argus and Peltier, 2010; Greenland: Tarasov and Peltier, 2002, 2004; the British Isles: Peltier, 2002; Shennan et al., 2002; Patagonia: Peltier, 2004; and Antarctica: Peltier, 2004), where each regional analysis is performed in a global context to yield a globally consistent response. In the most recent versions of the model, including the one used as an input to the CMIP5/PMIP3 composite ice sheet, satellite geodetic data (e.g. GPS, GRACE) is used to provide additional constraints (Peltier and Drummond, 2008; Argus and Peltier, 2010). ICE-4G (Peltier, 1994) was used to define the land-sea mask, the ice sheet extent and elevation, and land-surface topography and palaeo-ocean bathymetry in the first phase of PMIP (PMIP1) and ICE-5G (Peltier, 2004) in the second phase of PMIP (PMIP2). ICE-5G was improved relative to ICE-4G largely through the incorporation of revised information about the extent of the Eurasian ice sheets at the LGM from the QUEEN project (Svendsen et al., 1999; Mangerud et al., 2001, 2002; Svendsen et al., 2004b) and the use of gravity changes across North America from the GRACE satellite as an additional constraint.

ICE-6G (or more precisely ICE-6G version 2.0 VM5a T60 Rot) differs from previous inversions through more extensive use of geodetic data as a constraint, including e.g. the global positioning satellite (GPS), satellite laser ranging (SLR), Very Long Baseline

PMIP3 Ice sheet configuration

A. Abe-Ouchi et al.

Title Page

Abstract

Introduction

Conclusions

References

Tables

Figures

◀

▶

◀

▶

Back

Close

Full Screen / Esc

Printer-friendly Version

Interactive Discussion



PMIP3 Ice sheet configuration

A. Abe-Ouchi et al.

Title Page

Abstract

Introduction

Conclusions

References

Tables

Figures

◀

▶

◀

▶

Back

Close

Full Screen / Esc

Printer-friendly Version

Interactive Discussion



Interferometry (VLBI), and Doppler Orbitography and Radiopositioning Integrated by Satellite (DORIS). The model uses the VM5a mantle viscosity profile with an elastic lithosphere thickness of 60 km (T60). VM5a is a three-layer approximation of the VM2 T90 profile described by Peltier and Drummond (2008), in which the lithosphere consists of a 60 km thick elastic layer above a 40 km thick layer that is higher viscous. This modification was made to improve the fit of the model to observations of horizontal displacement rates in North America. ICE-6G also takes account of the Earth's rotational effect (Rot) on the geoid. The sea-level predictions from ICE-6G have been shown to provide a good fit to several hundred Holocene RSL curves (Argus and Peltier, 2010), including Holocene RSL observations for the Caribbean Sea and the Atlantic coast of North America (Engelhart et al., 2011; Toscano et al., 2011). Engelhart et al. (2011) showed that a further improvement to the match between observations and predictions for the southern part of the Atlantic coast could be obtained by reducing the viscosity on the upper mantle (above 660 km) from 0.5×10^{21} Pa s (VM5a) to 0.25×10^{21} Pa s (VM5b). However, subsequent work (Roy and Peltier, 2015). has shown that an even better match is obtained by reducing the viscosity of the upper part of the lower mantle.

2.2 GLAC-1a ice reconstruction

The GLAC-1a reconstruction is based on a set of glaciological models that are derived from a plausible climate forcing based on PMIP1 and PMIP2 results for LGM and that fit independently derived ice margin chronologies, within explicit uncertainties. The climate forcing involves an interpolation between present day observed climatologies and the set of highest resolution LGM fields from PMIP1 and PMIP2 data sets. The interpolation is weighted according to a glaciological inversion of the GRIP record (Tarasov and Peltier, 2003) for regional temperatures over the last glacial cycle.

The North American and Eurasian reconstructions are derived from separate Bayesian calibrations of the Glacial Systems Model (GSM). The GSM incorporates a 3-D thermo-mechanically coupled shallow ice-sheet model, a permafrost resolving bed thermal model, an asynchronously coupled down-slope surface drainage/lake depth

PMIP3 Ice sheet configuration

A. Abe-Ouchi et al.

Title Page

Abstract

Introduction

Conclusions

References

Tables

Figures

◀

▶

◀

▶

Back

Close

Full Screen / Esc

Printer-friendly Version

Interactive Discussion



5 solver, and also includes thermodynamic lake ice, sub-glacial till-deformation, buoyancy and temperature dependent ice calving, and an ice-shelf representation (Tarasov and Peltier, 2004, 2005, 2007; Tarasov et al., 2012). The visco-elastic bedrock response uses either the VM2 (as used in ICE-5G) or VM5a (used in ICE-6G) earth rheologies. RSL is computed using a gravitationally self-consistent formalism similar to that of Peltier (2009), except that it includes an eustatic approximation for dealing with changing ocean masks and does not take account of Earth rotational effects (Tarasov et al., 2012).

10 Separate calibrations are made for North America and Eurasia. The calibration involves 36 ensemble parameters for North America and 29 ensemble parameters for Eurasia, to capture uncertainties in deglacial climate and ice dynamics. The majority of these parameters are used for the climate forcing, including weighting the EOFs between PMIP models for LGM monthly precipitation and temperature, regional desert elevation effects, and LGM atmospheric lapse rate. Other ensemble parameters adjust the calving response, the effective viscosity of subglacial till, the strength of the ice-marginal constraint, and flow parameters for ice-shelves. Model runs are forced to stay within uncertainties of independently derived ice margin chronologies for North America (Dyke, 2004) and Eurasia (Hughes et al., 2014). Calibration targets include RSL observations from 512 sites (Tarasov and Peltier, 2002), geologically-inferred deglacial ice-margin chronologies, and geodetic constraints from Argus and Peltier (2010). In the case of North America, the calibrated ensemble is further scored with respect to strand-lines (paleo lake-level indicators) and observations of the maximum level of marine inundation. Model runs are penalised in proportion to the amount of margin forcing required, so the calibration is directed towards a climate forcing that is consistent with the margin chronology.

25 The model was originally calibrated using the ICE-4G ice load reconstruction for Antarctica and the VM2 Earth rheology. However, the subsequent use of an expanded geodetic data-set for North America coupled with the significant reduction in LGM Antarctic ice volume in ICE-6G v.2 compared to ICE-4G led to a significant misfit with

**PMIP3 Ice sheet
configuration**

A. Abe-Ouchi et al.

[Title Page](#)[Abstract](#)[Introduction](#)[Conclusions](#)[References](#)[Tables](#)[Figures](#)[I ◀](#)[▶ I](#)[◀](#)[▶](#)[Back](#)[Close](#)[Full Screen / Esc](#)[Printer-friendly Version](#)[Interactive Discussion](#)

the far-field Barbados RSL record. A random 2000 member ensemble was generated along with a rerun of the best 300 previously calibrated parameter sets and some 200 attempts at hand-tuning. There is a significant tradeoff between fitting the Barbados constraint and fitting the constraints from other locations. In order to satisfy the Barbados constraint, the 1.5 sigma upper limit of the previously calibrated ensemble for North America (which almost reaches the inferred Barbados record for 26 to 21 ka) was used. A weighted ensemble mean of the model runs that passed hard threshold constraints in the previous calibration was used for North America. The Eurasian calibration converged and was successful, except for minor issues with the Norwegian fjords. A single run with the largest 26 ka RSL contribution to the Barbados record was therefore used. A single run was chosen to ensure consistency between drainage fields and the surface topography. The Greenland model is from Tarasov and Peltier (2002, 2003), a glaciological model with hand-tuned climate adjustments to enforce fit to RSL records and the GRIP borehole temperature record.

2.3 ANU ice reconstruction

The ANU reconstruction has also evolved over a period of years in an iterative fashion (Lambeck and Johnston, 1998; Lambeck and Chappell, 2001; Lambeck et al., 2014). The first iterations were based on the analysis of far-field sea-level data, where the sea-level signal is predominantly a measure of the changes in total ice volume (the ice-volume equivalent sea level or ESL). The principle isostatic contribution to these sea levels is from the change in water load, a function of the rate at which water is added into or removed from the oceans and how it is distributed within ocean basins. Simple models were initially used for the ice sheets. The separation of mantle rheology from the ESL function was achieved by using the spatial variability of the far-field sea-level signals (Nakada and Lambeck, 1989). The resulting ice volume was then redistributed between the ice sheets using scaling relations initially and iterating between far-field and near-field solutions to ensure convergence (Lambeck et al., 2002, 2014).

PMIP3 Ice sheet configuration

A. Abe-Ouchi et al.

Title Page

Abstract

Introduction

Conclusions

References

Tables

Figures

◀

▶

◀

▶

Back

Close

Full Screen / Esc

Printer-friendly Version

Interactive Discussion



Inversions were also made for individual NH ice sheets using new compilations of field data from within and close to the ice margins, which are sensitive to the ice model and mantle rheology. Separate reconstructions have been made for Scandinavia (Lambeck et al., 1998, 2010), the Barents-Kara region (Lambeck, 1995a, 1996), Greenland (Fleming and Lambeck, 2004), the British Isles (Lambeck, 1993, 1995b), and North America (Lambeck, Purcell and Zhao, unpublished). These separate solutions allow lateral variability in mantle viscosity beneath the individual ice sheets to be detected, as well as differences between oceanic and continental mantle (Lambeck and Chapell, 2001). Some interactions occur between the separate ice sheet solutions requiring further iterations as each ice-sheet model is modified.

The field data from Antarctica is insufficient to use a similar approach to reconstruct ice-volume changes. Volume changes for the Antarctic ESL were obtained as the difference between the global ESL (Lambeck et al., 2014) and the NH ESL, the latter being the sum of the individual ice sheet contributions, and including mountain deglaciation in both hemispheres (Lambeck and Purcell, 2005). The ice in Antarctica was then distributed using the LGM ice margins proposed by Anderson et al. (2002), and assuming the ice profiles followed the quasi-parabolic function proposed by Paterson (1994). The retreat history is determined by the difference between the global ESL function and the combined northern-hemisphere mountain-glacier contributions. This reconstruction is not meant to be an accurate reflection of Antarctic ice history. Rather it is a convenient way of disposing of ice volume that cannot be attributed to the NH ice sheets in a way that does not impact in a major way on the far-field and NH analyses.

Several iterations have been performed to combine the far-field and individual ice-sheet reconstructions. The results used to create the CMIP5/PMIP3 composite are based on solutions current in 2009. The inversions yield changes in ice thickness compared to the present-day volume of each ice sheet. Thus, the LGM ice thickness is obtained by adding the present-day ice thickness. The LGM ice elevation, with respect to sea level at the LGM is obtained by subtracting the sea-level change (geoid change beneath the ice sheet) from the LGM ice thickness. The ESL function used in these

solutions is defined as all land ice and grounded ice on the shelves. The LGM ocean margin is defined by the ice-grounding line (Lambeck et al., 2003).

3 Construction of the composite CMIP5/PMIP3 ice sheets

3.1 Terminology

We use the term topography to refer to the altitude of the upper ice surface if the land is covered by ice, including floating ice, or the altitude of the land surface or ocean floor in areas not covered by ice or floating ice. Topography can be expressed either relative to modern sea level or relative to the sea level at a specific time t . We use $\text{Topo}(t)$ for topography relative to the sea level at time t , and $\text{topo}(t)$ for topography expressed relative to modern sea level (i.e. when t is 0).

Surface altitude (Surf) is the altitude of the bottom of the atmosphere. $\text{Surf}(t)$ is defined as:

$$\text{Surf}(t) = \max [0, \text{Topo}(t)], \quad (1)$$

which is 0 for ocean grid points and topography otherwise. Bathymetry (Bath) is the altitude of the ocean-floor under ice-shelves or topography otherwise.

There are four components that need to be provided to define ice-sheet related boundary conditions at the LGM: the difference in surface altitude (ΔSurf), an ice mask (Mask_1), an ice/shelf mask (Mask_2) and a land/sea mask (Mask_3). The first term (ΔSurf) is the difference in the surface altitude between LGM and the present-day. The three masks define the conditions at individual grid points. In the ice mask (Mask_1), 0 indicates ice-free and 1 indicates ice-covered grid points, including floating ice points. In the ice/shelf mask (Mask_2), 0 indicates ice-free points, 1 indicates grounded ice, and 2 indicates floating ice grid points. In the land/sea mask (Mask_3), 0 indicates land and 1 indicates ocean grid points. This information is provided for the domain from -180 to 179° in longitude and -89.5 to 89.5° in latitude, at a spatial resolution of $1^\circ \times 1^\circ$.

3.2 Conversion to common grid

The difference in the surface altitude at the LGM can be computed as:

$$\Delta\text{Surf}(21 \text{ ka}) = \text{Surf}(21 \text{ ka}) - \text{Surf}(0 \text{ ka}). \quad (2)$$

However, each of the individual ice-sheet reconstructions provides different outputs corresponding to the terms on the right hand side of this equation (Table 1). ANU provides estimates of the change in thickness between LGM and present day (ΔThick) and relative sea level (RSL), GLAC-1a provides Thick and $\text{topo}(21 \text{ ka})$, while ICE-6G provides $\text{Topo}(21 \text{ ka})$ and bathymetry $\text{Bath}(21 \text{ ka})$ as well as providing explicit masks for 21 and 0 ka. In order to produce the composite CMIP5/PMIP3 data set, it was therefore necessary to transform the original outputs before interpolating these data onto a common grid.

The domain of ICE-6G v2.0 is the same as that used in the composite CMIP5/PMIP3 reconstructions, so no spatial transformation was needed. The difference in the surface elevation at the LGM compared to the present day was computed from the original variables as:

$$\Delta\text{Surf}(21 \text{ ka}) = \max[0, \text{Topo}(21 \text{ ka})] - \max[0, \text{Topo}(0 \text{ ka})]. \quad (3)$$

The ice mask, $\text{Mask}_1(21 \text{ ka})$, was extracted directly from the original reconstruction. The ice/shelf mask, $\text{Mask}_2(21 \text{ ka})$, was computed from Topo and Bath as:

$$\text{Mask}_2(21 \text{ ka}) = \begin{cases} 2 & \text{if } \text{Topo} \neq \text{Bath}, \\ \text{Mask}_1 & \text{otherwise.} \end{cases} \quad (4)$$

The ANU reconstruction provides RSL and (ΔThick) for four separate regions (Table 1). RSL over the British Isles was computed under the assumption that the present-day is in equilibrium, with a mantle density of 4500 kg m^{-3} . These terms were first interpolated to the PMIP3 spatial grid, but no attempt was made to attribute values to gridpoints beyond those covered by the original data set.

Title Page

Abstract

Introduction

Conclusions

References

Tables

Figures

◀

▶

◀

▶

Back

Close

Full Screen / Esc

Printer-friendly Version

Interactive Discussion



PMIP3 Ice sheet configuration

A. Abe-Ouchi et al.

Title Page

Abstract

Introduction

Conclusions

References

Tables

Figures

I◀

▶I

◀

▶

Back

Close

Full Screen / Esc

Printer-friendly Version

Interactive Discussion



The LGM topography was computed as:

$$\text{Topo}(21 \text{ ka}) = \text{Topo}(0 \text{ ka}) + \Delta\text{Thick} - \text{RSL}, \quad (5)$$

where $\text{Topo}(0 \text{ ka})$ was derived from the ETOPO1 data set (Amante and Eakins, 2009). Ice-covered grid points that were still under 0 m (i.e. sea level elevation) after this procedure were corrected using an ice-floating adjustment, using ice and water densities 910 and 1028 kg m^{-3} respectively. Topography was then converted to ΔSurf using Eq. (3). There are several grid cells (e.g. near ice divides) where ice is present but $\Delta\text{Thick} = 0$. A modern reference ice mask is therefore required to compute the LGM ice mask for the ANU reconstruction. The LGM ice mask was therefore computed as:

$$\text{Mask}_1(21 \text{ ka}) = \begin{cases} 0 & \text{if Topo} \neq \text{Bath}, \\ 1 & \text{else if ICE-6GMask}_1 = 1, \\ 1 & \text{else if } \Delta\text{Thick}(21 \text{ ka}) > 0, \\ 0 & \text{otherwise.} \end{cases} \quad (6)$$

The ice/shelf mask was computed as:

$$\text{Mask}_2 = \begin{cases} 2 & \text{if Topo}(21 \text{ ka}) < 0, \\ 1 & \text{if Mask}_1 = 1, \\ 0 & \text{otherwise.} \end{cases} \quad (7)$$

The GLAC-1a reconstruction provide $\text{Thick}(21 \text{ ka})$ and $\text{topo}(21 \text{ ka})$ for North America and Eurasia, and specifies the global sea level change of 116 m. The topography relative to LGM sea level is computed as:

$$\text{Topo}(21 \text{ ka}) = \text{topo}(21 \text{ ka}) + 116 \text{ m}. \quad (8)$$

The resulting values were then interpolated to the PMIP3 grid, although no attempt was made to attribute values to gridpoints beyond those covered by the original data set (i.e. Antarctica). Gridpoints that were ice-covered but below sea level were corrected using

the same floating-ice adjustment as used for the ANU reconstruction. ΔSurf was then computed using Eq. (3). The ice mask was computed from Thick(21 ka) as:

$$\text{Mask}_1 = \begin{cases} 0 & \text{if Thick}(21 \text{ ka}) = 0, \\ 1 & \text{otherwise.} \end{cases} \quad (9)$$

The ice/shelf mask was computed using Eq. (7).

5 3.3 Integration of the three reconstructions

The CMIP5/PMIP3 composite ice-sheet reconstruction was created from the three transformed individual reconstructions. The LGM ice mask was taken as the maximum possible coverage:

$$\text{Mask}_1 = \begin{cases} 1 & \text{if at least one of the three Mask}_1 \text{ is } 1, \\ 0 & \text{otherwise.} \end{cases} \quad (10)$$

10 The surface altitude for ice-free grid cells was taken from ICE-6G v.2, while the difference in the surface altitude for ice-covered grid cells was computed by averaging the three reconstructions:

$$\Delta\text{Surf} = \begin{cases} (\Delta\text{Surf}'(\text{ANU}) + \Delta\text{Surf}'(\text{ICE-6G}) + \Delta\text{Surf}'(\text{GLAC-1}))/N_d & \text{where Mask}_{1,\text{ave}} = 1, \\ \Delta\text{Surf}(\text{ICE-6G}) & \text{otherwise,} \end{cases} \quad (11)$$

15 where N_d is the number of individual datasets (i.e. between 1 and 3) which provide a value for ΔSurf for a given grid-point, and $\Delta\text{Surf}'$ is the masked surface altitude such as:

$$\Delta\text{Surf}' = \begin{cases} \Delta\text{Surf} & \text{if defined,} \\ 0 & \text{if undefined (no quantity).} \end{cases} \quad (12)$$

The ice/shelf mask is computed as minimum possible shelf coverage.

$$\text{Mask}_2 = \begin{cases} 1 & \text{if at least one of the three Mask}_2 \text{ is } 1, \\ 0 & \text{if all of the three Mask}_2 \text{ are } 0, \\ 2 & \text{otherwise.} \end{cases} \quad (13)$$

The resulting mask had five glaciated grid points where ΔSurf was anomalously much lower than the surrounding points. We took the average value of the surrounding grid points, in order to avoid unrealistic spatial variability in ice-sheet topography. The present-day area of the Caspian Sea was included in the LGM land/sea mask, and a small number of land gridcells spuriously assigned to ocean were also corrected.

4 Comparison of the ice-sheet reconstructions

4.1 Comparison of the individual ice sheet reconstructions

The ANU reconstruction consistently shows the largest changes and GLAC-1a reconstruction the smallest changes in NH ice sheet volume (Table 2). The estimates for the Laurentide Ice Sheet, when expressed in terms of eustatic sea level, vary from 83 to 77 m, and the estimates for the Eurasian Ice Sheet from 18 to 14 m. The GLAC-1a reconstruction shows the Laurentide Ice Sheet as a single broad dome, with maximum elevations ($< 3000\text{m}$) in the west (Fig. 1). ICE-6G v.2 also shows maximum elevations in the western part of the ice sheet, but has a smaller secondary maximum over the James Bay area (Fig. 1). A larger part of the Laurentide Ice Sheet has elevations $> 3000\text{m}$ in the ANU reconstruction (Fig. 1). The GLAC-1a and ICE-6G v.2 reconstructions for Greenland are similar (because they are essentially derived from the same model: see Tarasov and Peltier, 2002, 2004) and show a flatter ice sheet with increased elevations around the margin and somewhat lower elevations than today in the centre (Fig. 2). The ANU reconstruction does not show lower central elevations, but does have an increase in marginal elevations. All three reconstructions show the

PMIP3 Ice sheet configuration

A. Abe-Ouchi et al.

Title Page

Abstract

Introduction

Conclusions

References

Tables

Figures



Back

Close

Full Screen / Esc

Printer-friendly Version

Interactive Discussion



Eurasian Ice Sheet with two major domes, one centred upon the Gulf of Bothnia and the other over the Barents Sea. The ANU reconstruction has elevations > 3000 m for the western dome, but both ICE-6G v.2 and GLAC-1a show similar and lower (2000–3000 m) elevations for both parts of the Eurasian Ice Sheet (Figs. 1, 2).

Only ICE-6G v.2 and ANU provide independent reconstructions of Antarctica. The volumetric change, when expressed in terms of eustatic sea level, is nearly twice as large in the ANU reconstruction (29 m) than in the ICE-6G v.2 reconstruction (15.6 m) (Table 2). More of the eastern part of the ice sheet lies at elevations > 3000 m in the ANU reconstruction (Fig. 3), whereas the ICE-6G v.2 reconstruction has a secondary dome at elevations > 3000 m over the Marie Byrd region which is not present in the ANU reconstructions. In both reconstructions, the major differences in elevation between the LGM and present are in western Antarctica, where elevation is higher by ca 900 m at the LGM than today (Fig. 4). The area of increased elevation is larger in the ANU reconstruction than in the ICE-6G v.2 reconstruction.

Although all of the individual reconstructions are constructed using information on the location of the margins of each ice sheet, nevertheless the final reconstructed extent of the ice sheets is derived from the inverse model. Thus, there may be discrepancies between the reconstructions and the actual, observed location of the LGM margins of each ice sheet. There are indeed differences between the ice and ice/shelf and land/sea masks obtained from each of the individual reconstructions. The implied change in eustatic sea level (Table 2) is larger in the ANU reconstruction than in the ICE-6G v.2 reconstruction. Similarly, the extent of ice shelves is consistently smaller in the ICE-6G v.2 reconstruction than in the ANU reconstruction, both for the NH and around Antarctica (Fig. 5).

4.2 Comparison of the CMIP5/PMIP3 composite reconstruction with earlier PMIP ice sheets

Ice sheet reconstructions used in the first two phases of PMIP were based on earlier versions of the ICE-6G inversion approach: ICE-4G (Peltier, 1994) for the first phase

PMIP3 Ice sheet configuration

A. Abe-Ouchi et al.

Title Page

Abstract

Introduction

Conclusions

References

Tables

Figures

◀

▶

◀

▶

Back

Close

Full Screen / Esc

Printer-friendly Version

Interactive Discussion



of PMIP (PMIP1) and ICE-5G (Peltier, 2004) for the second phase of PMIP (PMIP2). ICE-5G was improved relative to ICE-4G through the incorporation of revised information about the extent of the Eurasian ice sheets at the LGM from the QUEEN project (Svendsen et al., 1999; Mangerud et al., 2001, 2002; Svendsen et al., 2004b). ICE-6G differs from ICE-5G because of the inclusion of constraints based on satellite geodetic data as well as a more extensive data set of relative sea level changes. The differences between the three reconstructions are substantial. The PMIP2 NH ice sheets are considerably higher than the CMIP5/PMIP3 composite ice sheet while the PMIP1 NH ice sheets are lower than the CMIP5/PMIP3 composite and do not show the pronounced dome in the western part of the Laurentide (Figs. 1, 2). The Eurasian ice sheet is less extensive in the CMIP5/PMIP3 composite reconstruction than in the earlier reconstructions but maximum elevations are lower than in the earlier PMIP reconstructions. In contrast, the region of western Antarctica characterised by large changes (< 900 m) is more extensive in the CMIP5/PMIP3 composite reconstruction than in the earlier reconstructions, though this is partly due to the higher spatial resolution of the composite ice sheet compared to the earlier reconstructions.

4.3 Magnitude of CMIP5/PMIP3 composite ice-sheet forcing

The implied forcing resulting from the change in ice sheets and land-sea geography given by the CMIP5/PMIP3 composite is estimated using the Taylor et al. (2007) approximate partial-radiative perturbation method. The method is based on a simplified shortwave radiative model of the atmosphere. Surface absorption, atmospheric scattering and absorption are represented by means of three parameters that are diagnosed at each grid cell from surface and top-of-the-atmosphere fluxes and albedo. These parameters are different in each model and simulation, and reflect the properties of the radiative code in the individual models, and the differences of these terms in the different time periods. To quantify the effect of the change of each of these parameters, the parameters in the simple model are perturbed individually by the amount that they change in the climate response in order to compute the corresponding radiative

change. We adopted a two-sided approach, in which two estimates of the radiative change are made considering the control simulation and the palaeo-simulation in turn as a reference. According to these calculations, the forcing resulting from the ice-sheet change is between -1.85 and -3.49 W m^{-2} depending on the climate model (Table 3), while the overall change in forcing varies between -3.62 and -5.20 W m^{-2} . The difference in forcing in simulations using the CMIP/PMIP composite (Fig. 6) and the PMIP2 ice sheet is ca 1.0 W m^{-2} .

4.4 Impact of differences between the ice-sheet reconstructions on climate

To evaluate the impact of elevation differences between the individual ice sheets and the CMIP5/PMIP3 composite ice sheet on surface climate, we have run simulations with atmosphere-slab ocean version of the MIROC3 model assuming no change in ocean heat transport from the control run and no change in ocean mask. Using different ice sheet reconstructions has an impact on surface temperature over the ice sheets themselves, and in adjacent regions of the ocean (Arctic, North Atlantic, Southern Ocean), and a smaller impact over the Northern Hemisphere partly through the influence on atmospheric stationary wave (Fig. 7). The largest differences from the CMIP5/PMIP composite occur where the reconstructions differ in terms of the ice extent (e.g. between North America and Greenland) or altitude (e.g. western Antarctica, Scandinavian ice sheet). The ANU reconstruction produces slightly colder temperatures in the Arctic than either ICE-6G v.2 or GLAC-1a. The largest discrepancy occurs over Antarctica, where regional differences in temperature can be $> 6^\circ\text{C}$ between the simulations using the ICE-6G v.2 and ANU reconstructions (Fig. 7).

According to the MIROC simulations (Fig. 7), the overall impact of using the CMIP5/PMIP3 composite ice sheet in preference to any individual reconstruction is smaller than the difference between the CMIP5/PMIP3 composite and the ICE-5G ice sheet used in the PMIP2 simulations. Comparison of the multi-model ensemble from PMIP2 and CMIP5/PMIP3 (Fig. 8) shows that the decision to move to a new generation of ice sheet reconstructions has a large impact on simulated LGM climate, not only in

Title Page

Abstract

Introduction

Conclusions

References

Tables

Figures

◀

▶

◀

▶

Back

Close

Full Screen / Esc

Printer-friendly Version

Interactive Discussion



regions adjacent to the ice sheets but also over the ocean and in the tropics. Based on these ensemble results, the use of the CMIP5/PMIP3 composite ice sheet together with the development of climate models produces an increase in global mean annual temperature of ca 0.5°C compared to the PMIP2 experiments.

5 Discussion and conclusions

In an ideal world, there would be a consensus about the form of the LGM ice sheets and thus no need to reconstruct a composite set of ice-sheet related boundary conditions. In reality, information is still emerging about the details of ice-sheet margins at the LGM, retreat history lithologic constraints and so on, and thus existing reconstructions differ. It is useful to explore the consequences of differences between reconstructions through sensitivity experiments, but model-model intercomparison is facilitated by the use of a single set of boundary conditions, which then allows a focus on the role of structural differences between models. It is heartening that the differences between the individual reconstructions contributing to the composite are relatively small and have only a minor impact on simulated NH radiative forcing and temperatures.

The differences between the CMIP5/PMIP3 composite ice sheet and the ice sheets used in LGM simulations made during earlier phases of PMIP are not negligible. Braconnot et al. (2012) estimated that the difference between the implied land-sea mask from the PMIP2 and CMIP5/PMIP3 ice sheet would result in an additional 0.6 W m^{-2} forcing in the CMIP5/PMIP3 simulations, while the difference in ice-sheet height would result in temperatures ca 0.6°C warmer than in the PMIP2 experiments. We estimate that, in fact, the difference in forcing in simulations using the CMIP/PMIP composite and the PMIP2 ice sheet is ca 1.0 W m^{-2} and the average (ensemble) difference in global mean annual temperature is ca 0.5°C. The climate difference is non-negligible over the North Atlantic and over the continents of Northern Hemisphere both due to radiative forcing and the atmospheric circulation change in multi models as well as the MIROC model sensitivity test.

PMIP3 Ice sheet configuration

A. Abe-Ouchi et al.

Title Page

Abstract

Introduction

Conclusions

References

Tables

Figures

⏪

⏩

◀

▶

Back

Close

Full Screen / Esc

Printer-friendly Version

Interactive Discussion



PMIP3 Ice sheet configuration

A. Abe-Ouchi et al.

[Title Page](#)[Abstract](#)[Introduction](#)[Conclusions](#)[References](#)[Tables](#)[Figures](#)[I ◀](#)[▶ I](#)[◀](#)[▶](#)[Back](#)[Close](#)[Full Screen / Esc](#)[Printer-friendly Version](#)[Interactive Discussion](#)

Sensitivity experiments using the MIROC model show that the decision to use a composite ice sheet, rather than any of the existing ice-sheet realisations, does have an impact on simulated climate. The differences, however, are largely confined to the ice sheets themselves and adjacent oceans and basically reflect disagreements between the independent reconstructions about ice extent and/or altitude. The choice makes little difference to simulated temperatures beyond the ice-sheet margins. Nevertheless, over the ice sheets the differences in surface temperature can be large ($> 5^{\circ}\text{C}$) and this could have a non-negligible impact on other aspects of the surface climate (see e.g. Chavaillaz et al., 2013) and ocean circulation. Testing the response of a fully coupled atmosphere-ocean model to these three reconstructions is beyond the scope of the present paper, but we would anticipate larger changes than in the atmosphere-slab ocean experiments, notably through the impact of the different reconstructions on westerly winds over the North Atlantic which can, in turn, have an impact on the Atlantic Meridional Overturning Circulation (Ullman et al., 2014). Thus, it is important that the differences between the reconstructions are examined carefully so that better-constrained reconstructions are available for future PMIP analyses. However, simulations made with the composite CMIP5/PMIP3 ice sheet have more realistic temperatures over Antarctica, falling within or very close to the uncertainty range of estimates of the LGM cooling derived from ice core data, than the majority of PMIP2 simulations (Masson-Delmotte et al., 2013). While this may reflect model improvements to some extent, it would be unlikely to occur if the ice-sheet configuration in the CMIP5/PMIP3 simulations were substantially wrong.

There are discrepancies between the actual, observation margin of each ice sheet at the LGM and the margins reconstructed by inverse modelling. Furthermore, the way in which ice-sheet topography and extent are implemented varies between different climate models. Thus, there may be differences between the CMIP5/PMIP3 ice sheet mask and the mask used by an individual model (see e.g. Chavaillaz et al., 2013; Fig. 9). Both of these issues could be important in the processing of model outputs for model-model or data-model comparison. This is clearly an issue that needs to be

addressed more fully in the design of palaeo-simulations for the next phase of CMIP (CMIP6). Changes in palaeo-bathymetry, which is one output that can be obtained from the ice sheet models (e.g. ICE-6G v.2) have rarely been implemented in a coupled ocean-atmosphere model context. The implications of palaeo-bathymetry changes for ocean circulation could be important, and again this is an issue that could be addressed in the future design of palaeo-experiments.

Our knowledge of the LGM ice-sheet margins is continually improving, as are the models that are used to reconstruct the most likely distribution of ice mass, and indeed there have been updated reconstructions of LGM ice sheet configuration since the CMIP5/PMIP3 ice sheet was constructed. For example, the ICE-6G_C (VM5a) reconstruction is an updated version of the ICE-6G(VM5a) v2.0 model discussed here, and informed by a much richer data base of space geodetic information (Argus et al., 2014; Peltier et al., 2015). It is inevitable that there will be further changes in the future. What is imperative, then, is that a wider range of models conduct sensitivity tests to the impact of ice sheet configuration. This would make it possible to draw on the wealth of palaeoclimate data from beyond the ice sheets to evaluate, and perhaps even constrain, ice-sheet reconstructions.

The Supplement related to this article is available online at doi:10.5194/gmdd-8-4293-2015-supplement.

Acknowledgements. This paper is a contribution to the ongoing work on the Palaeoclimate Modelling Intercomparison Project. We thank Rosemarie Drummond, Jun'ici Okuno and Rumi Ohgaito for technical assistance.

PMIP3 Ice sheet configuration

A. Abe-Ouchi et al.

Title Page

Abstract

Introduction

Conclusions

References

Tables

Figures



Back

Close

Full Screen / Esc

Printer-friendly Version

Interactive Discussion



References

- Abe-Ouchi, A., Segawa, T., and Saito, F.: Climatic Conditions for modelling the Northern Hemisphere ice sheets throughout the ice age cycle, *Clim. Past*, 3, 423–438, doi:10.5194/cp-3-423-2007, 2007. 4298
- 5 Abe-Ouchi, A., Saito, F., Kawamura, K., Raymo, M. E., Okuno, J., Takahashi, K., and Blatter, H.: Insolation-driven 100,000-year glacial cycles and hysteresis of ice-sheet volume, *Nature*, 500, 190–193, doi:10.1038/nature12374, 2013. 4298
- Alyea, F.: Numerical simulation of an ice age paleoclimate, Atmospheric Science Paper No. 193, Colorado State University, Fort Collins, Colorado, USA, 1972. 4296
- 10 Amante, C. and Eakins, B.: ETOPO1 1 Arc-Minute Global Relief Model: Procedures, Data Sources and Analysis, NOAA Technical Memorandum NESDIS NGDC-24. National Geophysical Data Center, NOAA, Boulder, Colorado, USA, doi:10.7289/V5C8276M, 2009. 4306
- Anderson, J. B., Shipp, S. S., Lowe, A. L., Wellner, J. S., and Mosola, A. B.: The Antarctic Ice Sheet during the Last Glacial Maximum and its subsequent retreat history: a review, *Quaternary Sci. Rev.*, 21, 49–70, 2002. 4303
- 15 Argus, D. F. and Peltier, W. R.: Constraining models of postglacial rebound using space geodesy: a detailed assessment of model ICE-5G (VM2) and its relatives, *Geophys. J. Int.*, 181, 697–723, doi:10.1111/j.1365-246X.2010.04562.x, 2010. 4298, 4299, 4300, 4301
- Argus, D. F., Peltier, W. R., Drummond, R., and Moore, A. W.: The Antarctica component of postglacial rebound model ICE-6G_C (VM5a) based on GPS positioning, exposure age dating of ice thicknesses, and relative sea level histories, *Geophys. J. Int.*, 198, 537–563, doi:10.1093/gji/ggu140, 2014. 4314
- 20 Bartlein, P. J., Harrison, S. P., Brewer, S., Connor, S., Davis, B. A. S., Gajewski, K., Guiot, J., Harrison-Prentice, T. I., Henderson, A., Peyron, O., Prentice, I. C., Scholze, M., Seppa, H., Shuman, B., Sugita, S., Thompson, R. S., Viau, A. E., Williams, J., and Wu, H.: Pollen-based continental climate reconstructions at 6 and 21 ka: a global synthesis, *Clim. Dynam.*, 37, 775–802, doi:10.1007/s00382-010-0904-1, 2011. 4296
- 25 Braconnot, P., Otto-Bliesner, B., Harrison, S., Joussaume, S., Peterchmitt, J.-Y., Abe-Ouchi, A., Crucifix, M., Driesschaert, E., Fichet, Th., Hewitt, C. D., Kageyama, M., Kitoh, A., Laîné, A., Loutre, M.-F., Marti, O., Merkel, U., Ramstein, G., Valdes, P., Weber, S. L., Yu, Y., and Zhao, Y.: Results of PMIP2 coupled simulations of the Mid-Holocene and Last Glacial Maxi-
- 30

PMIP3 Ice sheet configuration

A. Abe-Ouchi et al.

Title Page

Abstract

Introduction

Conclusions

References

Tables

Figures

I ◀

▶ I

◀

▶

Back

Close

Full Screen / Esc

Printer-friendly Version

Interactive Discussion



mum – Part 1: experiments and large-scale features, *Clim. Past*, 3, 261–277, doi:10.5194/cp-3-261-2007, 2007. 4296

Braconnot, P., Otto-Bliesner, B., Harrison, S., Joussaume, S., Peterchmitt, J.-Y., Abe-Ouchi, A., Crucifix, M., Driesschaert, E., Fichet, Th., Hewitt, C. D., Kageyama, M., Kitoh, A., Loutre, M.-F., Marti, O., Merkel, U., Ramstein, G., Valdes, P., Weber, L., Yu, Y., and Zhao, Y.: Results of PMIP2 coupled simulations of the Mid-Holocene and Last Glacial Maximum – Part 2: feedbacks with emphasis on the location of the ITCZ and mid- and high latitudes heat budget, *Clim. Past*, 3, 279–296, doi:10.5194/cp-3-279-2007, 2007. 4296

Braconnot, P., Harrison, S. P., Kageyama, M., Bartlein, P. J., Masson-Delmotte, V., Abe-Ouchi, A., Otto-Bliesner, B., and Zhao, Y.: Evaluation of climate models using palaeoclimatic data, *Nature Clim. Change*, 2, 417–424, doi:10.1038/NCLIMATE1456, 2012. 4296, 4312, 4327

Brady, E. C., Otto-Bliesner, B. L., Kay, J. E., and Rosenbloom, N.: Sensitivity to glacial forcing in the CCSM4, *J. Climate*, 26, 1901–1925, doi:10.1175/JCLI-D-11-00416.1, 2013. 4296, 4297

Broccoli, A. J.: Tropical cooling at the last glacial maximum: an atmosphere-mixed layer ocean model simulation, *J. Climate*, 13, 951–976, doi:10.1175/1520-0442(2000)013<0951:TCATLG>2.0.CO;2, 2000. 4297

Broccoli, A. J. and Manabe, S.: The influence of continental ice, atmospheric CO₂, and land albedo on the climate of the last glacial maximum, *Clim. Dynam.*, 1, 87–99, doi:10.1007/BF01054478, 1987. 4297

Brovkin, V., Ganopolski, A., Archer, D., and Munhoven, G.: Glacial CO₂ cycle as a succession of key physical and biogeochemical processes, *Clim. Past*, 8, 251–264, doi:10.5194/cp-8-251-2012, 2012. 4298

Chavaillaz, Y., Codron, F., and Kageyama, M.: Southern westerlies in LGM and future (RCP4.5) climates, *Clim. Past*, 9, 517–524, doi:10.5194/cp-9-517-2013, 2013. 4313

Clark, P. U., Dyke, A. S., Shakun, J. D., Carlson, A. E., Clark, J., Wohlfarth, B., Mitrovica, J. X., Hostetler, S. W., and McCabe, A. M.: The last glacial maximum, *Science*, 325, 710–714, doi:10.1126/science.1172873, 2009. 4298

CLIMAP: Seasonal reconstructions of the Earth's surface at the last glacial maximum, no. MC-36 in Map Chart Series, Geological Society of America, Boulder, Colorado, 1981. 4297

CLIMAP Project Members: The surface of the Earth, *Science*, 191, 1131–1137, 1976. 4297

Collins, M., Knutti, R., Arblaster, J., Dufresne, J.-L., Fichet, T., Friedlingstein, P., Gao, X., Gutowski, W., Johns, T., Krinner, G., Shongwe, M., Tebaldi, C., Weaver, A., and Wehner, M.:

PMIP3 Ice sheet configuration

A. Abe-Ouchi et al.

Title Page

Abstract

Introduction

Conclusions

References

Tables

Figures

I◀

▶I

◀

▶

Back

Close

Full Screen / Esc

Printer-friendly Version

Interactive Discussion



Long-term climate change: projections, commitments and irreversibility, in: Climate Change 2013: The Physical Science Basis. Contribution of Working Group I to the Fifth Assessment Report of the Intergovernmental Panel on Climate Change, edited by: Stocker, T., Qin, D., Plattner, G.-K., Tignor, M., Allen, S., Boschung, J., Nauels, A., Xia, Y., Bex, V., and Midgley, P., Cambridge University Press, Cambridge, UK and New York, NY, USA, 2013. 4296

Dyke, A. S.: An outline of North American deglaciation with emphasis on central and northern Canada, in: Quaternary Glaciation — Extent and Chronology, Part II, edited by: Ehlers, J. and Gibbard, P. L., vol. 26 of Developments in Quaternary Science, 374–424, Elsevier, Amsterdam, the Netherlands, 2004. 4297, 4301

Dyke, A. S. and Prest, V. K.: Late Wisconsinan and Holocene history of the Laurentide ice sheet, Geogr. Phys. Quatern., 41, 237–263, doi:10.7202/032681ar, 1987. 4297

Ehlers, J., Gibbard, P. L., and Hughes, P. D.: Quaternary Glaciations-Extent and Chronology: A Closer Look, vol. 15, Elsevier, Amsterdam, the Netherlands, 2011. 4297

Engelhart, S. E., Peltier, W. R., and Horton, B. P.: Holocene relative sea-level changes and glacial isostatic adjustment of the U. S. Atlantic coast, Geology, 39, 751–754, 2011. 4299, 4300

Fleming, K. and Lambeck, K.: Constraints on the Greenland Ice Sheet since the Last Glacial Maximum from sea-level observations and glacial-rebound models, Quaternary Sci. Rev., 23, 1053–1077, doi:10.1016/j.quascirev.2003.11.001, 2004. 4303

Ganopolski, A. and Calov, R.: The role of orbital forcing, carbon dioxide and regolith in 100 kyr glacial cycles, Clim. Past, 7, 1415–1425, doi:10.5194/cp-7-1415-2011, 2011. 4298

Gates, W. L.: Modeling the Ice-Age climate, Science, 191, 1138–1144, doi:10.1126/science.191.4232.1138, 1976. 4296

Gyllencreutz, G., Mangerud, J., Svendsen, J.-I., and Lohne, Ø.: DATED – a GIS-based reconstruction and dating database of the Eurasian deglaciation, in: Applied Quaternary Research in the Central Part of Glaciated Terrain, edited by: Johansson, P. and Sarala, P., 113–120, Geological Survey of Finland, Espoo, Finland, 2007. 4297

Hargreaves, J. C., Abe-Ouchi, A., and Annan, J. D.: Linking glacial and future climates through an ensemble of GCM simulations, Clim. Past, 3, 77–87, doi:10.5194/cp-3-77-2007, 2007. 4296

Harrison, S. and Bartlein, P.: Records from the past, lessons for the future: what the palaeo-record implies about mechanisms of global change, in: The Future of the World's Climates,

PMIP3 Ice sheet configuration

A. Abe-Ouchi et al.

Title Page

Abstract

Introduction

Conclusions

References

Tables

Figures

◀

▶

◀

▶

Back

Close

Full Screen / Esc

Printer-friendly Version

Interactive Discussion



- edited by: Henderson-Sellers, A. and McGuffie, K., 403–436, Elsevier, Amsterdam, the Netherlands, 2012. 4296
- Hewitt, C. D. and Mitchell, J. F. B.: Radiative forcing and response of a GCM to ice age boundary conditions: cloud feedback and climate sensitivity, *Clim. Dynam.*, 13, 821–834, doi:10.1007/s003820050199, 1997. 4297
- Hughes, A., Mangerud, J., Gyllencreutz, R., Svendsen, J., and Lohne, O.: Evolution of the Eurasian Ice Sheets during the last deglaciation (25–10 kyr), Abstract, American Geophysical Union Fall Meeting, San Francisco, 13–19 December 2014, 2014. 4301
- Justino, F., Timmermann, A., Merkel, U., and Souza, E. P.: Synoptic reorganization of atmospheric flow during the last glacial maximum, *J. Climate*, 18, 2826–2846, doi:10.1175/JCLI3403.1, 2005. 4298
- Kim, S. J.: The effect of atmospheric CO₂ and ice sheet topography on LGM climate, *Clim. Dynam.*, 22, 639–651, doi:10.1007/s00382-004-0412-2, 2004. 4297
- Kirtman, B., Power, S. B., Adedoyin, A. J., Boer, G. J., Bojariu, R., Camilloni, I., Doblas-Reyes, F., Fiore, A. M., Kimoto, M., Meehl, G., Prather, M., Sarr, A., Schär, C., Sutton, R., van Oldenborgh, G. J., Vecchi, G., and Wang, H.-J.: Near-term climate change: projections and predictability, in: *Climate Change 2013: The Physical Science Basis. Contribution of Working Group I to the Fifth Assessment Report of the Intergovernmental Panel on Climate Change*, edited by: Stocker, T., Qin, D., Plattner, G.-K., Tignor, M., Allen, S., Boschung, J., Nauels, A., Xia, Y., Bex, V., and Midgley, P., Cambridge University Press, Cambridge, UK and New York, NY, USA, 2013. 4296
- Kutzbach, J. E. and Guetter, P. J.: The influence of changing orbital parameters and surface boundary conditions on climate simulations for the past 18 000 years, *J. Atmos. Sci.*, 43, 1726–1759, doi:10.1175/1520-0469(1986)043<1726:TIOCOP>2.0.CO;2, 1986. 4296
- Lambeck, K.: Glacial rebound of the British Isles—II. A high-resolution, high-precision model, *Geophys. J. Int.*, 115, 960–990, doi:10.1111/j.1365-246X.1993.tb01504.x, 1993. 4303
- Lambeck, K.: Late Pleistocene and Holocene sea-level change in Greece and south-western Turkey: a separation of eustatic, isostatic and tectonic contributions, *Geophys. J. Int.*, 122, 1022–1044, doi:10.1111/j.1365-246X.1995.tb06853.x, 1995a. 4303
- Lambeck, K.: Late Devensian and Holocene shorelines of the British-Isles and North-Sea from models of glacio-hydro-isostatic rebound, *J. Geol. Soc.*, 152, 437–448, 1995b. 4303
- Lambeck, K.: Limits on the areal extent of the Barents Sea ice sheet in Late Weichselian time, *Global Planet. Change*, 12, 41–51, doi:10.1016/0921-8181(95)00011-9, 1996. 4303

PMIP3 Ice sheet configuration

A. Abe-Ouchi et al.

Title Page

Abstract

Introduction

Conclusions

References

Tables

Figures

◀

▶

◀

▶

Back

Close

Full Screen / Esc

Printer-friendly Version

Interactive Discussion



- Lambeck, K. and Chappell, J.: Sea level change through the last glacial cycle, *Science*, 292, 679–686, doi:10.1126/science.1059549, 2001. 4302, 4303
- Lambeck, K. and Johnston, P.: The viscosity of the mantle: evidence from analyses of glacial rebound phenomena, in: *The Earth's Mantle*, edited by: Jackson, I., 461–502, Cambridge Univ. Press, Cambridge, 1998. 4302
- Lambeck, K. and Purcell, A.: Sea-level change in the Mediterranean Sea since the LGM: model predictions for tectonically stable areas, *Quaternary Sci. Rev.*, 24, 1969–1988, doi:10.1016/j.quascirev.2004.06.025, 2005. 4303
- Lambeck, K., Smither, C., and Johnston, P.: Sea-level change, glacial rebound and mantle viscosity for northern Europe, *Geophys. J. Int.*, 134, 102–144, doi:10.1046/j.1365-246x.1998.00541.x, 1998. 4303
- Lambeck, K., Yokoyama, Y., and Purcell, T.: Into and out of the last glacial maximum: sea-level change during oxygen isotope stages 3 and 2, *Quaternary Sci. Rev.*, 21, 343–360, doi:10.1016/S0277-3791(01)00071-3, 2002. 4302
- Lambeck, K., Purcell, A., Johnston, P., Nakada, M., and Yokoyama, Y.: Water-load definition in the glacio-hydro-isostatic sea-level equation, *Quaternary Sci. Rev.*, 22, 309–318, doi:10.1016/S0277-3791(02)00142-7, 2003. 4304
- Lambeck, K., Purcell, A., Zhao, J., and Svensson, N.-O.: The Scandinavian Ice Sheet: from MIS 4 to the end of the last glacial maximum, *Boreas*, 39, 410–435, doi:10.1111/j.1502-3885.2010.00140.x, 2010. 4298, 4303
- Lambeck, K., Rouby, H., Purcell, A., Sun, Y., and Sambridge, M.: Sea level and global ice volumes from the last glacial maximum to the Holocene, *P. Natl. Acad. Sci. USA*, 111, 15296–15303, doi:10.1073/pnas.1411762111, 2014. 4302, 4303
- Manabe, S. and Hahn, D. G.: Simulation of the tropical climate of an ice age, *J. Geophys. Res.*, 82, 3889–3911, doi:10.1029/JC082i027p03889, 1977. 4296
- Mangerud, J., Astakhov, V. I., Murray, A., and Svendsen, J. I.: The chronology of a large ice-dammed lake and the Barents-Kara Ice Sheet advances, Northern Russia, *Global Planet. Change*, 31, 321–336, doi:10.1016/S0921-8181(01)00127-8, 2001. 4299, 4310
- Mangerud, J., Astakhov, V., and Svendsen, J.-I.: The extent of the Barents-Kara ice sheet during the last glacial maximum, *Quaternary Sci. Rev.*, 21, 111–119, doi:10.1016/S0277-3791(01)00088-9, 2002. 4299, 4310

PMIP3 Ice sheet configuration

A. Abe-Ouchi et al.

Title Page

Abstract

Introduction

Conclusions

References

Tables

Figures

I ◀

▶ I

◀

▶

Back

Close

Full Screen / Esc

Printer-friendly Version

Interactive Discussion



Mangerud, J., Goehring, B. M., Lohne, Ø. S., Svendsen, J. I., and Gyllencreutz, R.: Collapse of marine-based outlet glaciers from the Scandinavian Ice Sheet, *Quaternary Sci. Rev.*, 67, 8–16, doi:10.1016/j.quascirev.2013.01.024, 2013. 4297

MARGO Project Members: Constraints on the magnitude and patterns of ocean cooling at the Last Glacial Maximum, *Nat. Geosci.*, 2, 127–132, doi:10.1038/ngeo411, 2009. 4296

Masson-Delmotte, V., Kageyama, M., Braconnot, P., Charbit, S., Krinner, G., Ritz, C., Guilyardi, E., Jouzel, J., Abe-Ouchi, A., Crucifix, M., Gladstone, R., Hewitt, C., Kitoh, A., LeGrande, A., Marti, O., Merkel, U., Motoi, T., Ohgaito, R., Otto-Bliesner, B., Peltier, W., Ross, I., Valdes, P., Vettoretti, G., Weber, S., Wolk, F., and Yu, Y.: Past and future polar amplification of climate change: climate model intercomparisons and ice-core constraints, *Clim. Dynam.*, 26, 513–529, doi:10.1007/s00382-005-0081-9, 2006. 4296

Masson-Delmotte, V., Schulz, M., Abe-Ouchi, A., Beer, J., Ganopolski, J., González Rouco, J., Jansen, E., Lambeck, K., Luterbacher, J., Naish, T., Osborn, T., Otto-Bliesner, B., Quinn, T., Ramesh, R., Rojas, M., Shao, X., and Timmermann, A.: Information from paleoclimate archives, in: *Climate Change 2013: The Physical Science Basis. Contribution of Working Group I to the Fifth Assessment Report of the Intergovernmental Panel on Climate Change*, edited by: Stocker, T., Qin, D., Plattner, G.-K., Tignor, M., Allen, S., Boschung, J., Nauels, A., Xia, Y., Bex, V., and Midgley, P., Cambridge University Press, Cambridge, UK and New York, NY, USA, 2013. 4296, 4313

Mickelson, D. and Colgan, P.: The southern Laurentide Ice Sheet in the United States: What have we learned in the last 40 years?, in: *Glacial Landscapes*, edited by: Evans, D. and Rea, B., 111–142, Erwin Arnold, London, 2003. 4297

Nakada, M. and Lambeck, K.: Late Pleistocene and Holocene sea-level change in the Australian region and mantle rheology, *Geophys. J.+*, 96, 497–517, 1989. 4302

Otto-Bliesner, B. L., Brady, E. C., Clauzet, G., Tomas, R., Levis, S., and Kothavala, Z.: Last glacial maximum and Holocene climate in CCSM3, *J. Climate*, 19, 2526–2544, doi:10.1175/JCLI3748.1, 2006. 4297, 4298

Paterson, W. S. B.: *The Physics of Glaciers*, 3rd edn., Pergamon, Oxford, 1994. 4303

Pausata, F. S. R., Li, C., Wettstein, J. J., Kageyama, M., and Nisancioglu, K. H.: The key role of topography in altering North Atlantic atmospheric circulation during the last glacial period, *Clim. Past*, 7, 1089–1101, doi:10.5194/cp-7-1089-2011, 2011. 4298

Peltier, W. R.: The impulse response of a Maxwell Earth, *Rev. Geophys. Space Ge.*, 12, 649–669, 1974. 4299

PMIP3 Ice sheet configuration

A. Abe-Ouchi et al.

Title Page

Abstract

Introduction

Conclusions

References

Tables

Figures

I ◀

▶ I

◀

▶

Back

Close

Full Screen / Esc

Printer-friendly Version

Interactive Discussion



- Peltier, W. R.: Glacial isostatic adjustment II: the inverse problem, *Geophys. J. Roy. Astr. Soc.*, 46, 669–706, 1976. 4299
- Peltier, W. R.: Ice age paleotopography, *Science*, 265, 195–201, 1994. 4297, 4299, 4309
- Peltier, W. R.: On eustatic sea level history: last glacial maximum to Holocene, *Quaternary Sci. Rev.*, 21, 377–396, 2002. 4299
- Peltier, W. R.: Global glacial isostasy and the surface of the Ice-Age Earth: the ICE-5G(VM2) model and GRACE, *Annu. Rev. Earth Pl. Sc.*, 32, 111–149, 2004. 4297, 4299, 4310
- Peltier, W. R.: Closure of the budget of global sea level rise over the GRACE era: the importance and magnitudes of the required corrections for global glacial isostatic adjustment, *Quaternary Sci. Rev.*, 28, 1658–1674, doi:10.1016/j.quascirev.2009.04.004, 2009. 4301
- Peltier, W. R. and Andrews, J. T.: Glacial isostatic adjustment I: the forward problem, *Geophys. J. Roy. Astr. Soc.*, 46, 605–646, 1976. 4299
- Peltier, W. R. and Drummond, R.: Rheological stratification of the lithosphere: a direct inference based upon the geodetically observed pattern of the glacial isostatic adjustment of the North American continent, *Geophys. Res. Lett.*, 35, L16314, doi:10.1029/2008GL034586, 2008. 4299, 4300
- Peltier, W. R., Argus, D. F., and Drummond, R.: Space geodesy constrains ice age terminal deglaciation: the global ICE-6G_C (VM5a) model, *J. Geophys. Res.-Sol. Ea.*, 120, 450–487, doi:10.1002/2014JB011176, 2014JB011176, 2015. 4314
- Prentice, I. C., Jolly, D., and BIOME 6000 participants: Mid-Holocene and glacial-maximum vegetation geography of the northern continents and Africa, *J. Biogeogr.*, 27, 507–519, doi:10.1046/j.1365-2699.2000.00425.x, 2000. 4296
- Roy, K. and Peltier, W.: Glacial isostatic adjustment, relative sea level history and mantle viscosity: reconciling relative sea level model predictions for the U.S. East coast with geological constraints, *Geophys. J. Int.*, 201, 1156–1181, doi:10.1093/gji/ggv066, 2015. 4300
- Schmidt, G. A., Annan, J. D., Bartlein, P. J., Cook, B. I., Guilyardi, E., Hargreaves, J. C., Harrison, S. P., Kageyama, M., LeGrande, A. N., Konecky, B., Lovejoy, S., Mann, M. E., Masson-Delmotte, V., Risi, C., Thompson, D., Timmermann, A., Tremblay, L.-B., and Yiou, P.: Using palaeo-climate comparisons to constrain future projections in CMIP5, *Clim. Past*, 10, 221–250, doi:10.5194/cp-10-221-2014, 2014. 4296
- Schmittner, A., Urban, N. M., Shakun, J. D., Mahowald, N. M., Clark, P. U., Bartlein, P. J., Mix, A. C., and Rosell-Melé, A.: Climate sensitivity estimated from temperature reconstruc-

PMIP3 Ice sheet configuration

A. Abe-Ouchi et al.

Title Page

Abstract

Introduction

Conclusions

References

Tables

Figures

I ◀

▶ I

◀

▶

Back

Close

Full Screen / Esc

Printer-friendly Version

Interactive Discussion



tions of the last glacial maximum, *Science*, 334, 1385–1388, doi:10.1126/science.1203513, 2011. 4296

Shennan, I., Peltier, W., Drummond, R., and Horton, B.: Global to local scale parameters determining relative sea-level changes and the post-glacial isostatic adjustment of Great Britain, *Quaternary Sci. Rev.*, 21, 397–408, doi:10.1016/S0277-3791(01)00091-9, {EPILOG}, 2002. 4299

Simpson, M. J. R., Milne, G. A., Huybrechts, P., and Long, A. J.: Calibrating a glaciological model of the Greenland ice sheet from the last glacial maximum to present-day using field observations of relative sea level and ice extent, *Quaternary Sci. Rev.*, 28, 1631–1657, doi:10.1016/j.quascirev.2009.03.004, 2009. 4297

Svendsen, J. I., Astakhov, V. I., Bolshiyakov, D. Y., Demidov, I., Dowdeswell, J. A., Gataullin, V., Hjort, C., Hubberten, H. W., Larsen, E., Mangerud, J., Melles, M., Möller, P., Saarnisto, M., and Siegert, M. J.: Maximum extent of the Eurasian ice sheets in the Barents and Kara Sea region during the Weichselian, *Boreas*, 28, 234–242, doi:10.1111/j.1502-3885.1999.tb00217.x, 1999. 4299, 4310

Svendsen, J. I., Alexanderson, H., Astakhov, V. I., Demidov, I., Dowdeswell, J. A., Funder, S., Gataullin, V., Henriksen, M., Hjort, C., Houmark-Nielsen, M., Hubberten, H. W., Ingolfsson, O., Jakobsson, M., Kjaer, K. H., Larsen, E., Lokrantz, H., Lunkka, J. P., Lysa, A., Mangerud, J., Matiouchkov, A., Murray, A., Moller, P., Niessen, F., Nikolskaya, O., Polyak, L., Saarnisto, M., Siegert, C., Siegert, M. J., Spielhagen, R. F., and Stein, R.: Late quaternary ice sheet history of northern Eurasia, *Quaternary Sci. Rev.*, 23, 1229–1271, 2004a.

Svendsen, J. I., Gataullin, V., Mangerud, J., and Polyak, L.: The glacial history of the Barents and Kara Sea Region, in: *Quaternary Glaciations Extent and Chronology Part I: Europe*, edited by: Ehlers, J. and Gibbard, P., vol. 2, Part 1 of *Developments in Quaternary Sciences*, 369–378, Elsevier, Amsterdam, the Netherlands, doi:10.1016/S1571-0866(04)80086-1, 2004b. 4299, 4310

Tarasov, L. and Peltier, W. R.: Greenland glacial history and local geodynamic consequences, *Geophys. J. Int.*, 150, 198–229, doi:10.1046/j.1365-246X.2002.01702.x, 2002. 4299, 4301, 4302, 4308

Tarasov, L. and Peltier, W. R.: Greenland glacial history, borehole constraints, and Eemian extent, *J. Geophys. Res.*, 108, 2143, doi:10.1029/2001JB001731, 2003. 4300, 4302

PMIP3 Ice sheet configuration

A. Abe-Ouchi et al.

Title Page

Abstract

Introduction

Conclusions

References

Tables

Figures

◀

▶

◀

▶

Back

Close

Full Screen / Esc

Printer-friendly Version

Interactive Discussion



- Tarasov, L. and Peltier, W. R.: A geophysically constrained large ensemble analysis of the deglacial history of the North American ice-sheet complex, *Quaternary Sci. Rev.*, 23, 359–388, doi:10.1016/j.quascirev.2003.08.004, 2004. 4299, 4301, 4308
- Tarasov, L. and Peltier, W. R.: Arctic freshwater forcing of the Younger Dryas cold reversal, *Nature*, 435, 662–665, doi:10.1038/nature03617, 2005. 4301
- Tarasov, L., and Peltier, W. R.: Coevolution of continental ice cover and permafrost extent over the last glacial-interglacial cycle in North America, *J. Geophys. Res.*, 112, F02S08, doi:10.1029/2006JF000661, 2007. 4301
- Tarasov, L., Dyke, A. S., Neal, R. M., and Peltier, W. R.: A data-calibrated distribution of deglacial chronologies for the North American ice complex from glaciological modeling, *Earth Planet. Sc. Lett.*, 315–316, 30–40, doi:10.1016/j.epsl.2011.09.010, 2012. 4298, 4301
- Taylor, K. E., Crucifix, M., Braconnot, P., Hewitt, C. D., Doutriaux, C., Broccoli, A. J., Mitchell, J. F. B., and Webb, M. J.: Estimating shortwave radiative forcing and response in climate models, *J. Climate*, 20, 2530–2543, doi:10.1175/JCLI4143.1, 2007. 4310
- Taylor, K. E., Stouffer, R. J., and Meehl, G. A.: An overview of CMIP5 and the experiment design, *B. Am. Meteorol. Soc.*, 93, 485–498, doi:10.1175/BAMS-D-11-00094.1, 2011. 4296
- Toscano, M. A., Peltier, W. R., and Drummond, R.: ICE-5G and ICE-6G models of post-glacial relative sea-level history applied to the Holocene coral reef record of northeastern St Croix, U. S. V. I.: investigating the influence of rotational feedback on GIA processes at tropical latitudes, *Quaternary Sci. Rev.*, 30, 3032–3042, 2011. 4300
- Tushingham, A. M. and Peltier, W. R.: ICE-3G: a new global model of late Pleistocene deglaciation based upon geophysical predictions of post-glacial relative sea level change, *J. Geophys. Res.*, 96, 4497–4523, 1991. 4299
- Ullman, D. J., LeGrande, A. N., Carlson, A. E., Anslow, F. S., and Licciardi, J. M.: Assessing the impact of Laurentide Ice Sheet topography on glacial climate, *Clim. Past*, 10, 487–507, doi:10.5194/cp-10-487-2014, 2014. 4298, 4313
- Vettoretti, G. and Peltier, W. R.: Last glacial maximum ice sheet impacts on North Atlantic climate variability: the importance of the sea ice lid, *Geophys. Res. Lett.*, 40, 6378–6383, doi:10.1002/2013GL058486, 2013GL058486, 2013. 4298
- Williams, J., Barry, R. G., and Washington, W. M.: Simulation of the atmospheric circulation using the NCAR global circulation model with Ice Age boundary conditions, *J. Appl. Meteorol.*, 13, 305–317, doi:10.1175/1520-0450(1974)013<0305:SOTACU>2.0.CO;2, 1974. 4296

Yoshimori, M., Yokohata, T., and Abe-Ouchi, A.: A comparison of climate feedback strength between CO₂ doubling and LGM experiments, *J. Climate*, 22, 3374–3395, doi:10.1175/2009JCLI2801.1, 2009. 4296

5 Yoshimori, M., Hargreaves, J. C., Annan, J. D., Yokohata, T., and Abe-Ouchi, A.: Dependency of feedbacks on forcing and climate state in physics parameter ensembles, *J. Climate*, 24, 6440–6455, doi:10.1175/2011JCLI3954.1, 2011. 4296

GMDD

8, 4293–4336, 2015

PMIP3 Ice sheet configuration

A. Abe-Ouchi et al.

Title Page

Abstract

Introduction

Conclusions

References

Tables

Figures

◀

▶

◀

▶

Back

Close

Full Screen / Esc

Printer-friendly Version

Interactive Discussion



PMIP3 Ice sheet configuration

A. Abe-Ouchi et al.

Table 2. Implied changes in ice volume for the Laurentide, Eurasian and Antarctic Ice Sheets, expressed in terms of impact on eustatic sea level (in m). The impact of eustatic sea level is inferred by assuming no change in ocean area compared to today (assumed ocean area: 360 768 576 km²), and using densities for ice and water of 910 and 1028 kg m⁻³ respectively. Results are shown for the three individual reconstructions (ICE-6Gv.2, GLAC-1a, ANU) and for the composite CMIP5/PMIP3 ice sheets, and compared to the implied changes for the ice sheets used in the Last Glacial Maximum simulations run in the first and second phases of the Palaeoclimate Modelling Intercomparison Project (PMIP1, PMIP2).

| | North America | Eurasia | Antarctica | Total |
|-----------------------|---------------|---------|-------------------|---------------|
| ICE-6Gv.2 | 76.8 | 17.5 | 15.6 | 113.0 |
| GLAC-1a | 76.6 | 14.0 | Not reconstructed | Not available |
| ANU | 82.5 | 18.2 | 29.0 | 130.0 |
| CMIP5/PMIP3 composite | 78.6 | 16.6 | 22.3 | 121.5 |
| PMIP1(ICE-4G) | 60.5 | 29.1 | 21.7 | 117.8 |
| PMIP2(ICE-5Gv1.1) | 74.6 | 20.3 | 17.3 | 112.2 |

Title Page

Abstract

Introduction

Conclusions

References

Tables

Figures

I ◀

▶ I

◀

▶

Back

Close

Full Screen / Esc

Printer-friendly Version

Interactive Discussion



PMIP3 Ice sheet configuration

A. Abe-Ouchi et al.

Table 3. Change in radiative forcing associated with changes in ice sheet and implied changes in land-sea geography, calculated for the CMIP5/PMIP3 composite and the PMIP2 ice sheets respectively. The resulting change in temperature (Δt_{as}) is also shown. The error is calculated as the difference between the estimates obtained while using the present day climate as a reference or the glacial climate as a reference in the partial-radiative perturbation calculation. Note that the values given for the PMIP2 ice sheet are slightly different from those given in Braconnot et al. (2012) because of corrections made subsequent to the publication of that paper. Values given here may also differ slightly from published results of individual models where either a different method or a different time window was used for the calculation.

| Climate model | Ice sheet | Ice sheet change | Land-sea change | Combined change | Δt_{as} (°C) |
|---------------------|-------------|------------------|------------------|------------------|----------------------|
| CCSM4 | CMIP5/PMIP3 | -2.47 ± 0.10 | -1.33 ± 0.00 | -3.79 ± 0.10 | -4.91 |
| IPSL-CM5A-LR | CMIP5/PMIP3 | -3.11 ± 0.15 | -1.79 ± 0.05 | -4.90 ± 0.20 | -4.60 |
| MIROC-ESM | CMIP5/PMIP3 | -3.45 ± 0.51 | -1.75 ± 0.19 | -5.20 ± 0.70 | -5.00 |
| MPI-ESM-P | CMIP5/PMIP3 | -3.49 ± 0.62 | -1.08 ± 0.06 | -4.57 ± 0.68 | -4.41 |
| MRI-CGCM3 | CMIP5/PMIP3 | -1.85 ± 0.10 | -1.77 ± 0.02 | -3.62 ± 0.12 | -4.68 |
| CCSM3 | PMIP2 | -1.85 ± 0.12 | -0.88 ± 0.00 | -2.72 ± 0.12 | -4.51 |
| CNRM | PMIP2 | -2.25 ± 0.32 | -0.74 ± 0.01 | -2.98 ± 0.32 | -3.05 |
| HadCM3M2_oa | PMIP2 | -2.55 ± 0.40 | -1.19 ± 0.11 | -3.73 ± 0.51 | -5.11 |
| HadCM3M2_oavM3M2_oa | PMIP2 | -2.72 ± 0.45 | -1.27 ± 0.12 | -3.98 ± 0.57 | -5.86 |
| IPSL-CM4 | PMIP2 | -2.43 ± 0.11 | -1.17 ± 0.03 | -3.60 ± 0.13 | -3.79 |
| MIROC3.2 | PMIP2 | -2.76 ± 0.54 | -0.78 ± 0.12 | -3.54 ± 0.66 | -3.70 |

Title Page

Abstract

Introduction

Conclusions

References

Tables

Figures

I ◀

▶ I

◀

▶

Back

Close

Full Screen / Esc

Printer-friendly Version

Interactive Discussion



PMIP3 Ice sheet configuration

A. Abe-Ouchi et al.

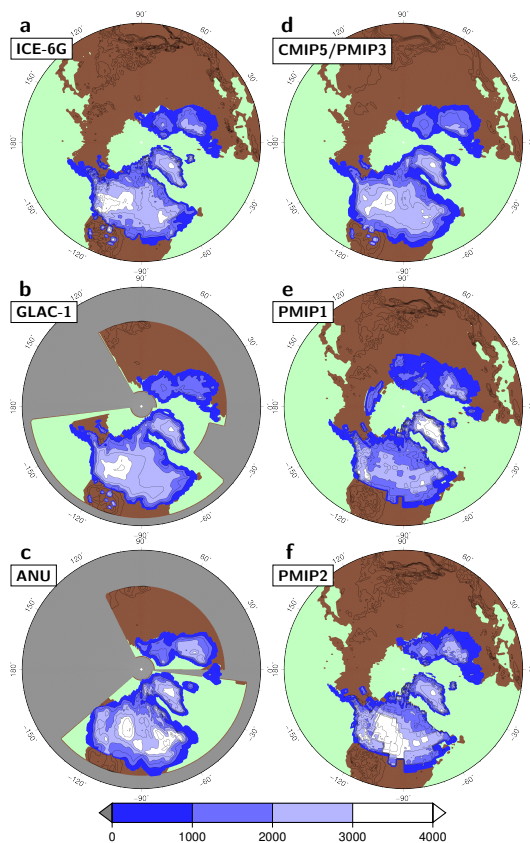


Figure 1. Surface elevation (m) at the Last Glacial Maximum (LGM) Northern Hemisphere ice sheets from the (a) ICE-6Gv.2, (b) GLAC-1a and (c) ANU reconstructions, and for (d) the CMIP5/PMIP3 composite compared to the ice sheets used in (e) PMIP1 and (f) PMIP2.

Title Page

Abstract

Introduction

Conclusions

References

Tables

Figures

I ◀

▶ I

◀

▶

Back

Close

Full Screen / Esc

Printer-friendly Version

Interactive Discussion



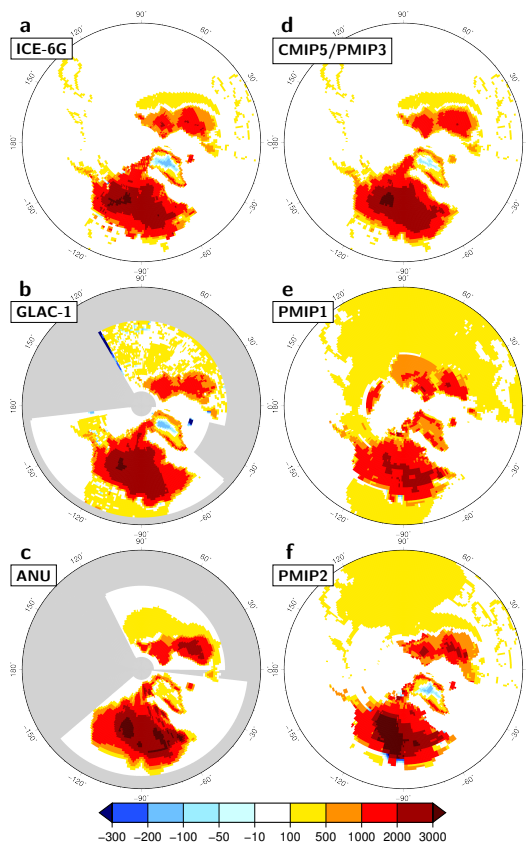


Figure 2. Difference in surface elevation (m) of the Northern Hemisphere ice sheets at the LGM compared to the present-day from the (a) ICE-6Gv.2, (b) GLAC-1a and (c) ANU reconstructions, and for (d) the CMIP5/PMIP3 composite compared to the ice sheets used in (e) PMIP1 and (f) PMIP2. The region shown is between 40 and 90° N .

PMIP3 Ice sheet configuration

A. Abe-Ouchi et al.

Title Page

Abstract

Introduction

Conclusions

References

Tables

Figures

◀

▶

◀

▶

Back

Close

Full Screen / Esc

Printer-friendly Version

Interactive Discussion



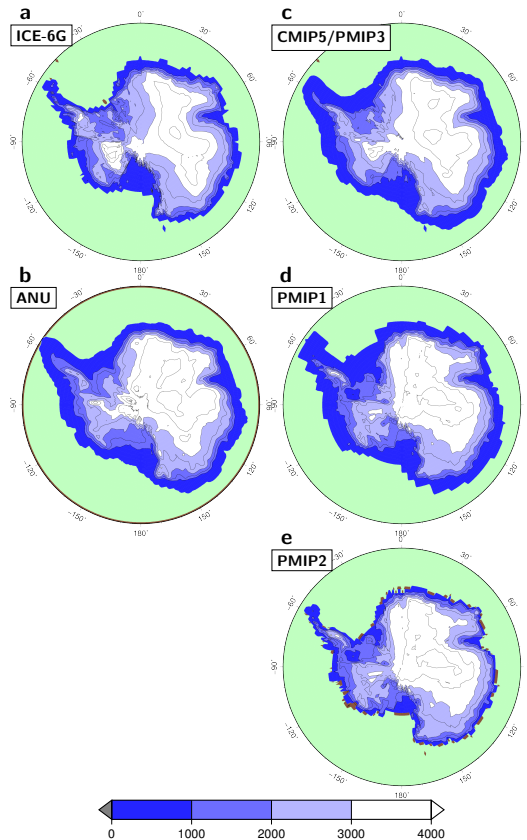


Figure 3. Surface elevation (m) of Antarctica at the LGM from the (a) ICE-6Gv.2, (b) ANU reconstructions, and for (c) the CMIP5/PMIP3 composite compared to the ice sheets used in (d) PMIP1 and (e) PMIP2. The GLAC-1a reconstruction for Antarctica is identical to that of ICE-6G, and is therefore not shown.

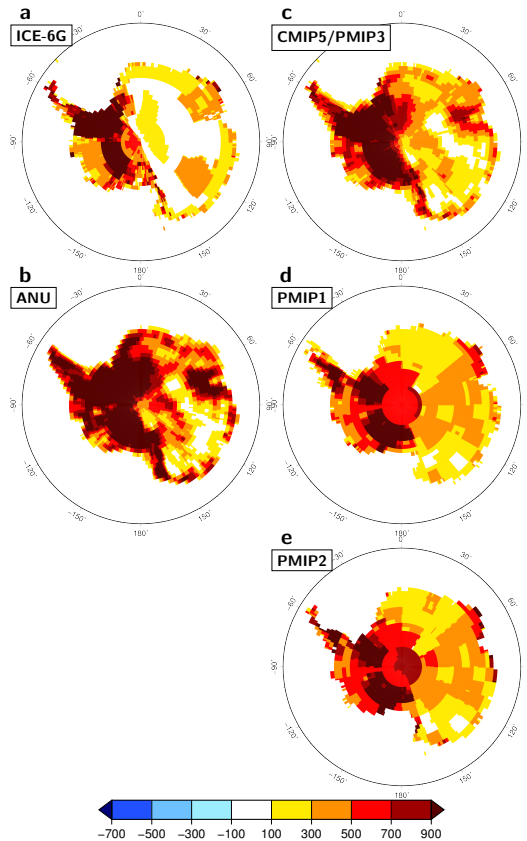


Figure 4. Difference in surface elevation (m) of Antarctica at the LGM compared to the present-day from the (a) ICE-6Gv.2, (b) ANU reconstructions, and for (c) the CMIP5/PMIP3 composite compared to the ice sheets used in (d) PMIP1 and (e) PMIP2. The GLAC-1a reconstruction for Antarctica is identical to that of ICE-6G, and is therefore not shown.

PMIP3 Ice sheet configuration

A. Abe-Ouchi et al.

Title Page

Abstract Introduction

Conclusions References

Tables Figures

⏪ ⏩

◀ ▶

Back Close

Full Screen / Esc

Printer-friendly Version

Interactive Discussion



PMIP3 Ice sheet configuration

A. Abe-Ouchi et al.

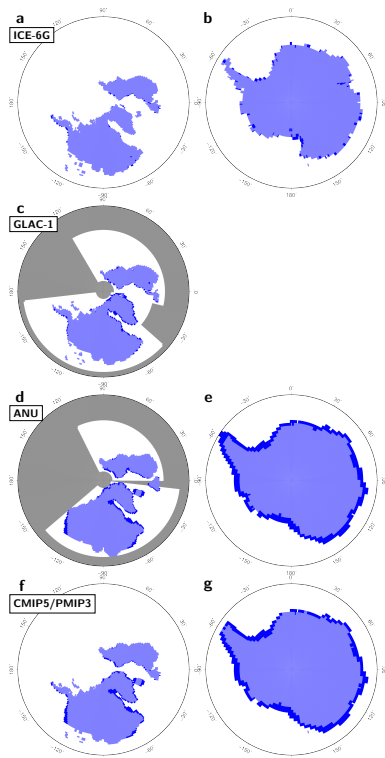


Figure 5. Ice/shelf extent at the LGM from the ice/shelf masks for the Northern Hemisphere derived from ICE-6Gv.2 for (a) the Northern Hemisphere and (b) Antarctica, from GLAC-1a (c) for the Northern Hemisphere, and from ANU for (d) the Northern Hemisphere and (e) Antarctica. The GLAC-1a reconstruction for Antarctica is identical to that of ICE-6Gv.2, and is therefore not shown. These reconstructed masks can be compared with the CMIP5/PMIP3 mask for (f) the Northern Hemisphere and (g) Antarctica. Cyan, blue and white areas indicate the grounded-ice, floating-ice and ice-free region, respectively.

Title Page

Abstract

Introduction

Conclusions

References

Tables

Figures

I ◀

▶ I

◀

▶

Back

Close

Full Screen / Esc

Printer-friendly Version

Interactive Discussion



PMIP3 Ice sheet configuration

A. Abe-Ouchi et al.

Title Page

Abstract

Introduction

Conclusions

References

Tables

Figures

◀

▶

◀

▶

Back

Close

Full Screen / Esc

Printer-friendly Version

Interactive Discussion

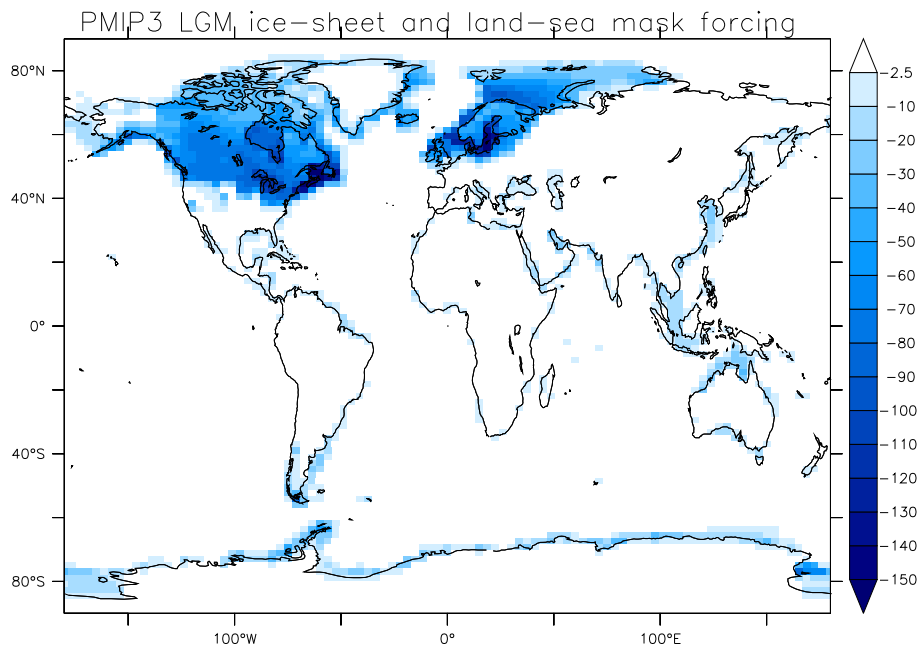


Figure 6. Estimation of the difference in radiative forcing and feedbacks at the LGM compared with pre-industrial conditions caused by imposition of the CMIP5/PMIP3 ice sheet and the change in the land-sea mask. The map is a composite of the results from five ocean-atmosphere models showing the spatial patterns of the change in total forcing associated with the expanded Northern Hemisphere ice sheets at the LGM and with the increase of land area due to lowered sea level.

PMIP3 Ice sheet configuration

A. Abe-Ouchi et al.

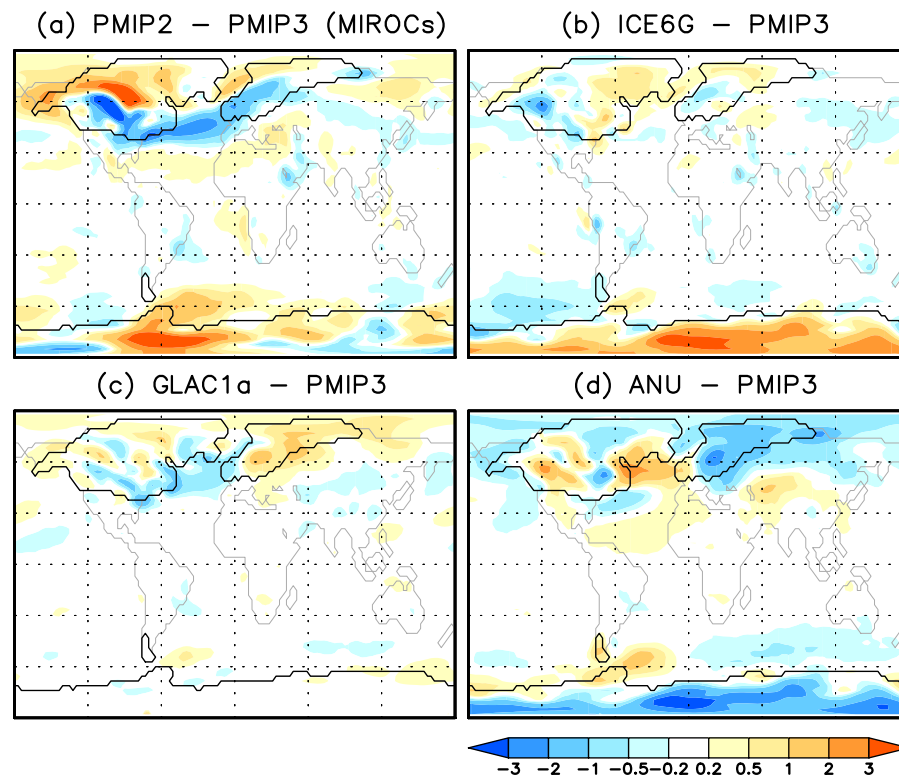


Figure 7. Impact of ice sheet choice on mean annual temperature (MAT) in simulations made with the MIROC slab ocean model. The plots show (a) MAT in the simulation with the CMIP5/PMIP3 composite ice sheet (CMIP5/PMIP3), (b) differences between this reference simulation and simulations made with (b) ICE-6Gv.2, (c) GLAC-1a, and (d) ANU. The land mask (> 50% land) is shown in grey, the ice margin (> 50% ice) is shown in black on all four plots.

Title Page

Abstract

Introduction

Conclusions

References

Tables

Figures

I◀

▶I

◀

▶

Back

Close

Full Screen / Esc

Printer-friendly Version

Interactive Discussion



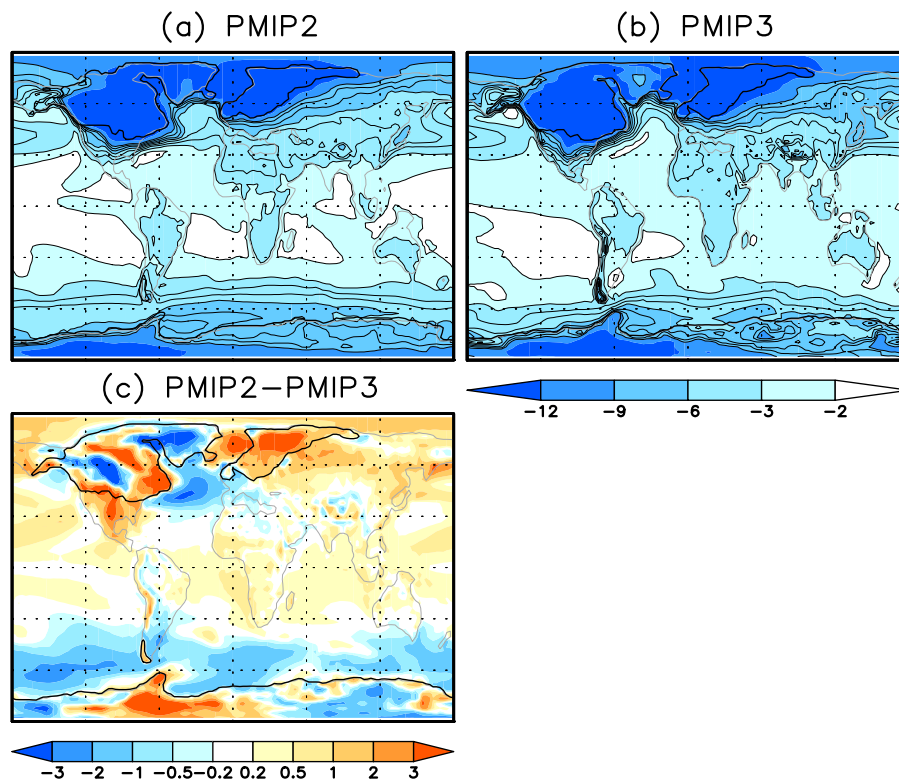


Figure 8. Change in mean annual temperature (MAT) in the (a) PMIP2 and (b) CMIP5/PMIP3 coupled ocean-atmosphere simulations. Each of these plots is an ensemble average of all the LGM simulations in PMIP2 and CMIP5/PMIP3 respectively. The difference between the ensemble mean results for the two generations of experiments is shown in plot (c). The land and ice masks are the same as Fig. 7. Contour lines are also illustrated in (a, b). The contour interval is 1°C where the temperature is higher than -9°C .

PMIP3 Ice sheet configuration

A. Abe-Ouchi et al.

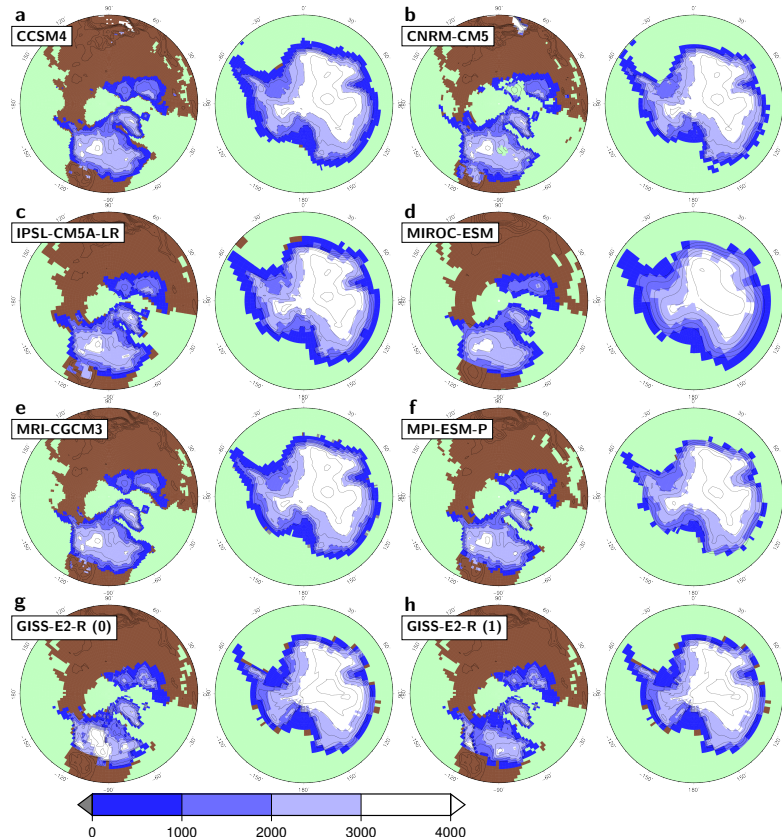


Figure 9. Implementation of the CMIP5/PMIP3 composite ice sheet in individual models. These plots show that there are small differences in prescribed ice sheet between models because of differences in e.g. model type and resolution.

Title Page

Abstract

Introduction

Conclusions

References

Tables

Figures

I ◀

▶ I

◀

▶

Back

Close

Full Screen / Esc

Printer-friendly Version

Interactive Discussion

